Local Stratopause Temperature Variabilities and their Embedding in the Global Context

Ronald Eixmann[1], Vivien Matthias[2], Gerd Baumgarten[1], Michael Gerding[1], and Josef Höffner[1]

[1]Leibniz Institute of Atmospheric Research, Schloss-Strasse 6, 18225 Kühlungsborn, Germany
[2]Potsdam Institute for Climate Impact Research, Telegrafenberg A 31, 14473 Potsdam, Germany

Correspondence: Ronald Eixmann (eixmann@iap-kborn.de)

Abstract. The stratopause is by definition the transition between the stratosphere and mesosphere. During winter the circulation in the stratosphere is mainly driven by quasi stationary planetary waves (PW) while the circulation in the mesosphere is mainly driven by gravity waves (GW). The question arises whether PWs or GWs dominate the variability of the stratopause. The most famous and dramatic variability of the middle atmosphere is a sudden stratospheric warming (SSW) generated by

5 PWs interacting with the polar vortex. A similar phenomenon but smaller in magnitude and more regional are stratopause temperature enhancements (STE) initially observed by local measurements and generated by breaking PWs. Thus it seems that PWs dominate the variability of the stratopause. In this study we want to quantify to which amount quasi stationary PWs contribute to the stratopause variability. To do that we combine local lidar observations at Kühlungsborn (54°N, 11°E) and Andenes (69°N, 16°E) with global MERRA-2 reanalysis data bringing the local variability of the stratopause into the global

10 context. Therefore we compare the temperature time series at Kühlungsborn and Andenes at 2 hPa, the altitude where STEs maximize, with characteristics (amplitude and phase) of PWs with wavenumbers 1, 2 and 3. We found that for Kühlungsborn 97% and for Andenes 98% of the local day-to-day variability of the stratopause can be explained by the variability of PWs with wavenumber 1, 2, and 3. Thus, the winter stratopause day-to-day variability is highly dominated by the variability of PWs.

1 Introduction

15 Upper stratosphere/lower mesosphere (USLM) temperatures are a sensitive indicator for climate change (Rind et al., 1998). Especially during winter dynamical changes of the USLM influence the entire stratosphere (Hitchman et al., 1989) via the downward control principle (Haynes et al., 1991) and that in turn can affect our tropospheric weather and climate (Baldwin et al., 2001; Kodera et al., 2008; Kretschmer et al., 2018).

The stratopause represents by definition the transition between the stratosphere and mesosphere. During winter the polar

20 stratosphere is characterised by a strong circumpolar westerly wind, known as the polar vortex. The polar vortex is disturbed in the northern hemisphere by planetary Rossby waves (PW) generated in the troposphere and propagating upward under westerly wind conditions into the middle atmosphere (Charney and Drazin, 1961; Matsuno, 1970). The strongest PWs that occur in the winter middle atmosphere are quasi stationary PWs (Matsuno, 1970). When those waves break they deposit their momentum in the middle atmosphere (McIntyre and Palmer, 1983) and thus driving especially the stratosphere away from

its radiative equilibrium by generating a mean meridional circulation from equator to pole with downward motion at the pole which adiabatically warms the polar stratosphere (e.g., Plumb, 2002; Manney et al., 2008). In the mesosphere the main driver of the circulation are gravity waves (GW) by implementing a mean meridional circulation from the summer to the winter pole with accompanied upward motion in summer and downward motion in winter resulting in a warmer winter mesosphere than

5 expected from the radiative equilibrium (Fritts and Alexander, 2003). Thus the variability of the stratopause seems to depend on the variability of PWs and GWs.

The most famous disturbance of the winter polar middle atmosphere triggered by PWs is the sudden stratospheric warming (SSW) which is characterized by a dramatic warming of the stratosphere and a simultaneous cooling of the mesosphere (Matsuno, 1971; Andrews et al., 1987; Matthias et al., 2012). A similar phenomenon that is smaller in magnitude and more

10 regional is the "stratopause temperature enhancement (STE)" (Meriwether and Gerrard, 2004) also known as "stratopause warming" (Braesicke and Langematz, 2000) or "USLM disturbance" (Manney et al., 2008; Thayer et al., 2010; Greer et al., 2013). While the term USLM disturbance often refers to the whole 3-D structure of the disturbance, the term STE refers to the observable temperature increase of the stratopause. In this study we will use the term STE since we focus on the variability of the stratopause temperature here.

15 Greer et al. (2013) investigated the mean characteristics of STE by constructing a climatology of these events using 20 years of stratospheric assimilated data from the U.K. Meteorological Office (UKMO). They found that STE occur between November and March in the northern hemisphere winter with a pronounced preference in December and preferentially over Northeastern Russia and Scandinavia. The mean duration of a STE is 8 days. In earlier observations STE occurred always shortly before a SSW (von Zahn et al., 1998) but later on there was evidence that STE do not necessarily develop into a SSW

20 (Meriwether and Gerrard, 2004; Manney et al., 2008). Greer et al. (2013) showed that in their assimilated model data all major SSW were preceded by a STE while that was the case only for half of the minor SSW. Approximately one third of all STE did not develop into a SSW at all. Similar to SSW, there is often a mesospheric cooling around 75 km associated with the STE (Meriwether and Gerrard, 2004; Thayer et al., 2010). Until now it is not completely understood how STEs develop. Several authors investigated the formation of STE using models (Fairlie et al., 1990; Braesicke and Langematz, 2000), reanalysis data

25 (Greer et al., 2013) or global satellite data (Thayer et al., 2010). The common sense is that PWs interact with the polar vortex in the upper stratosphere leading to an ageostrophic circulation driving vertical motions resulting in adiabatic heating in the upper stratosphere and cooling in the mesosphere due to the induced change in the vertical propagation of gravity waves. There is evidence that this perturbation may grow through baroclinic instability (Fairlie et al., 1990; Thayer et al., 2010; Greer et al., 2013) which is fed off by strong upward propagating PWs between 10 and 2 hPa (Thayer et al., 2010; Greer et al., 2013).

30 So in general the main cause for stratopause day-to-day variabilities seem to be PWs. In this study we want to quantify to which amount quasi stationary PWs contribute to the stratopause day-to-day variability at one location. Therefore we combine local lidar measurements with global reanalysis data. Lidar observations are performed in Andenes (69°N, 16°E) and Kühlungsborn (54°N, 11°E) whereby Andenes is located mostly within the polar vortex and Kühlungsborn at the edge of the polar vortex (see Greer et al. (2013) their Fig. 5). These two locations are especially suited for this kind of study since they lie in the

35 area where STE can occur (Greer et al., 2013). MERRA-2 reanalysis data will be used to investigate the temporal variability of

the stratopause of the last 38 winter (1980/81 - 2018/19). The paper is structure as follows: in section 2 the two lidar systems and the MERRA-2 reanalysis data are briefly described as well as the methods applied in this study. Our results are described in section 3, discussed in section 4 and summarized in section 5.

2   Data and methods

5   To bring the local variability of the stratopause into the global context we combine local lidar measurements at two locations at high and mid-latitudes with global reanalysis data of MERRA-2. The local lidar measurements are used to characterize STEs and to roughly estimate the quality of local MERRA-2 profiles. Using the temporal evolution of MERRA-2 reanalysis data at these two locations and the corresponding latitudes, the variability at one location is compared with the global variation of PWs regarding their amplitude and phase.

10   ### 2.1   Local lidar observations

In this study we mainly use Rayleigh/Mie/Raman (RMR) lidar systems which are located at the ALOMAR observatory near Andenes in the Norwegian Arctic (69°N,16°E) and at Kühlungsborn in Germany (54°N, 11°E). The climatology of each station comprises ten years of measurements between 2002 and 2012 in winter between December and February. For the calculation of the temperature from the RMR lidar raw data we use the hydrostatic density integration as described, e.g., by Chanin and
15   Hauchecorne (1981), based on the backscatter at 532 nm wavelength.

The ALOMAR RMR lidar is able to obtain temperatures from above the stratospheric aerosol layer (i.e. above ∼22–34 km depending on actual conditions) up to ∼90 km during both darkness and daylight conditions. The lidar is actually a twin lidar system with two independent lasers (∼20 W average power at 532 nm) and two tiltable telescopes of 1.8 m diameter. Typical integration times for this study are 1 h at 2.5 km vertical resolution. Further details about the ALOMAR RMR lidar are
20   described by Baumgarten (2010) and Schöch et al. (2008).

The RMR lidar at Kühlungsborn is similar to the system at ALOMAR. An additional detection channel for N_2 vibrational Raman backscatter at 608 nm allows for the correction of stratospheric aerosol effects. By this, the lowest altitude bins for Rayleigh temperature retrieval can be set to 22 km. The ∼20 W average power at 532 nm and the four receiver telescopes of 60 cm diameter each allow for 1 km vertical resolution after 1 h integration. Typically, the upper altitude limit is above 85 km
25   altitude. In this study the data are limited to nighttime conditions. The RMR lidar data at Kühlungsborn is complemented by temperature profiles obtained by a collocated potassium resonance lidar. This technique provides absolute temperatures between ∼85 and 105 km by probing the Doppler broadening of the D1 resonance line of potassium atoms that exist in this altitude range. These data are also used as a start value for the hydrostatic temperature retrieval for the Kühlungsborn RMR lidar, while the calculation for the ALOMAR RMR lidar is initialised with climatological data. Further details of the
30   temperature lidars at Kühlungsborn are described by Alpers et al. (2004) and Gerding et al. (2008).

Note that in this study only nighttime measurements (Andenes: 134, Kühlungsborn: 71) with at least three hours of measurement are taken into account from both lidar systems. A nighttime mean of the lidar temperature profiles is calculated to minimize the impact of small scale effects.

2.2 Global MERRA-2 reanalysis data

5 To set local stratopause variabilities into the global context we use global reanalysis data from the Modern-Era Retrospective analysis for Research and Applications Version 2 (MERRA-2; Gelaro et al. (2017); Bosilovich et al. (2015); Molod et al. (2015)). Here we use daily means of the 3-hourly instantaneous output on 42 constant pressure levels ranging from 1000 hPa to 0.1 hPa, i.e. from the surface up to 68 km. The horizontal resolution is 0.625 degree in longitude and 0.5 degree in latitude. For our analysis we use MERRA-2 reanalysis data from winter 1980/81 to 2018/19, i.e. 38 winter in total whereas the term

10 winter includes the months December, January and February.

2.3 Methods

Here we use the regional variability STE to investigate the agreement between the local lidar measurements and the global MERRA-2 reanalysis data. Similar to Thayer et al. (2010) and Greer et al. (2013) we identify a STE if the temperature profile is at least 15 K above the climatological mean at 2 hPa (near the stratopause). To calculate the deviation from the climatological

15 mean for the lidar nighttime temperatures the NRLMSISE-00 empirical model of the atmosphere (Picone et al., 2002) is used as a reference atmosphere. This model comprises an all-embracing day by day temperature climatology. Thus the deviation from the climatological mean for the lidar temperature data is calculated by subtracting the NRLMSISE-00 model climatology from the nighttime lidar measuerement for each altitude, day and location separately. Consequently we can divide the lidar nighttime temperatures into STE and non-STE.

20 The deviation from the climatological mean in MERRA-2 data is calculated by removing the long term mean computed from the 38 winters of MERRA-2 data, for each day, altitude and longitude separately at the latitudes where Kühlungsborn and Andenes are located. Note that daily mean values are used for MERRA-2 data and nighttime means are used for lidar data. Thus an impact of tides especially on the lidar data can not be excluded.

To bring the local values at Andenes and Kühlungsborn into the global context regarding PWs, the three predominant

25 zonal wavenumbers 1, 2 and 3 are fitted to the MERRA-2 data at both latitudes separately. The following description is illustrated in Fig. 1: for each day the original daily mean data (blue line) at each latitude at 2 hPa is decomposed into the three dominating wavenumbers 1, 2 and 3 (green line for wave 1, orange line for wave 123, i.e. all three waves together) using a least-squares procedure. Thus we somewhat reconstructed the original data based on the different PW components. Here we call the maximum absolute value of a wave the *amplitude* of that wave and the value between zero and an arbitrary location

30 on the wave the *local displacement*. In this study the local displacement is at 11°E for Kühlungsborn and 16°E for Andenes respectively. With the help of these two concepts (amplitude and local displacement) not only the change in the amplitude of a PW but also the change in phase of the wave. For example, the amplitude of a PW remains the same but changes in phase and thus can change the value of the local displacement at Andenes.
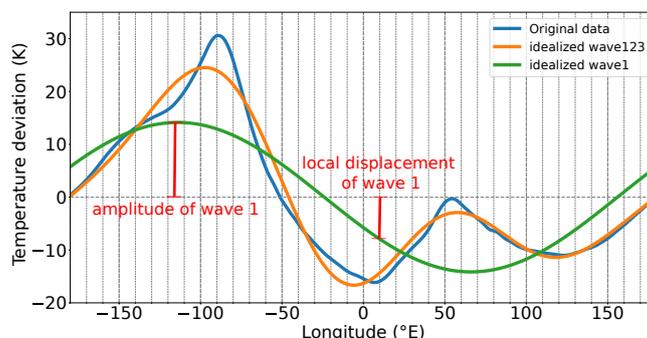
Figure 1. Illustration of the decomposition of the original time series into wave number 1, 2 and 3 and of the concept of amplitude and local displacement which denotes the value at a specific longitude.

Following this approach we reconstruct the whole time series for Andenes (69°N, 16°E) and Kühlungsborn (54°N, 11°E) based on PWs with wave numbers 1, 2 and 3. To visualize the differences and similarities of the original time series and the reconstructed time series we correlate them for each location separately (i.e. Kühlungsborn and Andenes) as will be shown in the next section.

3 Results

Before we compare the temporal evolution of local stratopause temperatures with the temporal evolution of PWs at the same altitude and latitude, we study the vertical profile of STEs using lidar data and compare the results with profiles of MERRA-2 reanalysis data.

3.1 Characteristics of vertical profiles of STEs from lidar measurements

Figure 2 shows all available winter nighttime mean profiles between 2002 and 2012 for Andenes (a) and Kühlungsborn (b) and those identified as STE (c, d). Thus profiles in c) and d) are a subset of a) and b), respectively. If one compares the long-term mean profiles (red line) of Andenes and Kühlungsborn in Fig. 2 a) and b), it is noticeable that the altitude of the stratopause is 4 km lower at Kühlungsborn (47 km) than at Andenes (51 km). The stratopause altitude during a STE is about 3 km lower at Kühlungsborn and 7 km lower at Andenes than the corresponding mean stratopause altitude. Possible causes for the difference in height of the stratopause between mid- and high latitudes as well as between STE and the long-term mean are discussed in section 4.

3.2 Comparison of lidar observations and MERRA-2 reanalysis data

Figure 3 a) and b) show vertical profiles of STEs (grey lines) and their average (red line) from MERRA-2 reanalysis data between winter 1980/81 and 2018/19 as well as the climatology for all available 38 winter (blue line). The climatological

stratopause altitude (cf. blue line) is 57 km at Andenes and about 49 km at Kühlungsborn and thus higher compared to the lidar data at both locations (50 km / 47 km respectively). However similar to the lidar data the stratopause is in general higher at Andenes than at Kühlungsborn. During the winter month between 2002 and 2012 we identified (not shown) 150 STE profiles for Andenes and 202 for Kühlungsborn. STEs occur in 14%/17% of all winter days ($38 \cdot 90 = 3420$) at Andenes/Kühlungsborn.

5 The reason why we define STEs at 2 hPa can be seen in Fig. 3 c) and d), showing again vertical profiles of STEs but with subtracted climatology. In general a STE ranges between 35 and 55 km with its maximum around 43 km which is in good agreement to findings of Meriwether and Gerrard (2004) and Greer et al. (2013).

The above described small differences between lidar measurements and MERRA-2 reanalysis data can have several causes. One reason is the higher temporal and vertical resolutions of the lidar measurements at higher altitudes in comparison to

10 MERRA-2 data. Local and especially small scale processes that are only parametrized in MERRA-2 can be captured by lidar measurements. Another one is the different number of profiles used for the calculation of the climatology. For the MERRA-2 climatology $38 \cdot 90 = 3420$ profiles were used in the calculation, while for the lidar data only 134 for Andenes and 71 for Kühlungsborn are available. Thus the number of profiles used for the climatologies and long term means is one magnitude smaller for lidar data than for MERRA-2 data. Furthermore the profiles are nighttime averages for the lidar data and daily

15 means for the MERRA-2 reanalysis data. Thus lidar temperature profiles are biased by solar tides and gravity waves with longer periods. When averaging nighttime measurements with a length of at least 3 hours, then only a part of a tide or gravity wave is averaged out. This effect is much weaker in MERRA-2 data since a daily mean is calculated here. Thus especially the bias from the solar tides is much weaker since the entire oscillation is used in the averaging process. The same arguments can be applied to the small differences of the STE-only climatologies between the lidar measurements and the MERRA-2 reanalysis

20 data since we have much more profiles included in the calculation for the MERRA-2 STE-climatology (478/584) than in the lidar data (41/20). However, all in all lidar and MERRA-2 data are in a good agreement and hence MERRA-2 reanalysis data can be used to bring local observations into the global context.

3.3   Local variability embedded into the global context

To bring local variability into the global context we compare the time series at Andenes and Kühlungsborn) at 2 hPa with the

25 time series from the amplitude of wave number 1, 2, 3 and 123 (all together) at the same latitude and with the time series of the local displacement for this very location (also for wave number 1, 2, 3 and 123).

Figure 4 shows the original time series at one location at 2 hPa (blue line), the time series of the amplitude for the respective PWs (green line) and the reconstructed time series (orange line) based on the respective PW (local displacement). This is done for Andenes (left column) and Kühlungsborn (right column) and for the different wave numbers (each row represents a

30 different wave number). The embedding of the local variability into the global context is exemplary shown for winter 2009/10. A similar analysis for all available 38 winters can be found in the supplement.

First, focusing on wave 123 for Andenes and Kühlungsborn, it is evident that the blue and the orange lines lay almost perfectly on top of each other. The correlation coefficient of the original and reconstructed time series for winter 2009/10 is 0.99 for Andenes and 0.97 for Kühlungsborn. Thus 99% of the day-to-day variability of the temperature at Andenes can be

	Andenes	Kühlungsborn
wave 123	0.98	0.97
wave 1	0.86	0.79
wave 2	0.64	0.75
wave 3	0.31	0.5

Table 1. Correlation coefficients between the original time series and the reconstructed time series for all available winters for Andenes and Kühlungsborn.

explained by the variability of PWs with wave number 1, 2 and 3. The correlation of the original time series with the amplitude (green line) results in correlation coefficients of almost zero for Andenes and only 0.27 for Kühlungsborn. The discrepancy between the correlation coefficients of the amplitude and local displacement results from the fact that the amplitude describes only the increase and decrease of the amplitude of the respective PW while the local displacement also takes the change in

5   phase into account. This can be observed especially well around day 0 in Kühlungsborn (upper row in Fig. 4). While the amplitude increases, the value of the local displacement decreases dramatically, due to the shift in phase of the waves. Around day -10, Kühlungsborn lies under the positive part of the wave packet where the temperature maximises. In the next 10 days, the phase shifts in such a way that Kühlungsborn is now located under the minimum half of the wave packet where the temperature minimises. The amplitude is blind to such a phase shift event explaining its much lower correlation coefficient.

10   During other occasions, for example between day -10 and 10 in Andenes, the amplitude and local displacement values are much more synchronous pointing to a stationary phase. Due to the much better description of the local variability by the local displacement or reconstructed time series (orange line) we will focus on this in the following.

Considering the individual wave numbers the largest correlation coefficient between the original time series and the reconstructed time series occurs for wave 1 at both locations (Andenes: $r_A = 0.9$, Kühlungsborn: $r_K = 0.84$). Thus wave number

15   1 dominates the variability of the winter stratopause. In both stations wave 2 ($r_A = 0.75, r_K = 0.74$) is slightly less important than wave 1 ($r_A = 0.9, r_K = 0.84$). Wave 3 plays by far the smallest role ($r_A = 0.5, r_K = 0.65$).

Similar to the example winter 2009/10 described in detail above we correlated the original time series of all available winters with the reconstructed time series of every individual wave number as well as all wave numbers together. The individual correlation coefficients for both locations can be found in table 1. In general 98% (97%) of the stratopause variability at

20   Andenes (Kühlungsborn) can be explained by the variability of PWs with wavenumber 1, 2 and 3. Also the other characteristics of the individual wavenumbers found in winter 2009/10 can be generalized. Note that we conducted this analysis also to temperature time series at 1 hPa, the climatological stratopause altitude at Kühlungsborn, and received the same results (not shown).

4 Discussion

As shown in Fig. 2 and 3 the stratopause is about 4 km lower at Kühlungsborn than at Andenes in the climatological mean. This phenomenon of an elevated and warmer winter stratopause at high latitudes compared to mid-latitudes was also observed by Hitchman et al. (1989) using global satellite measurements. Combining these global satellite observations with a 2-D model

5 they found evidence that the elevated polar stratopause is caused by GWs driving a meridional circulation with downwelling over the winter pole. The mean residual meridional circulation is characterised by downwelling in the middle atmosphere resulting in adiabatic warming and differs between the stratosphere and mesosphere in its driving mechanism. While it is driven by PWs in the stratosphere (e.g., Andrews et al., 1987; Plumb, 2002), it is driven by GWs in the mesosphere (e.g., Lindzen, 1981; Plumb, 2002). The stratopause is by definition the transition between these two atmospheric layers. However, Haynes

10 et al. (1991) showed that the mean meridional circulation at any level is determined by the vertically integrated momentum forcing above that level. Garcia and Boville (1994) confirmed the significant contribution of GWs in the mesosphere on the circulation in the stratosphere at high latitudes by using a simple numerical model in the middle atmosphere with parametrized GW and PW breaking. Removing the GW breaking in their model results in a significant colder stratosphere and less downwelling at high latitudes during winter. Thus the difference in the stratopause altitude between mid- and high latitudes can be

15 explained by the mean meridional circulation in the high latitudes mesosphere driven by GWs .

The altitude of the stratopause is lower during STEs than in the climatology for both locations (cf. Fig. 2 and 3). This decreased altitude of the stratopause during STEs was also observed by earlier studies (von Zahn et al., 1998; Meriwether and Gerrard, 2004). The formation of a STE and thus also the descent of the stratopause is explained by several authors (Fairlie

20 et al., 1990; Thayer et al., 2010; Greer et al., 2013) as follows: interactions between the polar vortex and PWs can be associated by localized momentum forcing resulting in a synoptic ageostrophic circulation which is accompanied with a strong vertical motion. This vertical motion points downward in the upper stratosphere, adiabatically warming this region and therefore descending the stratopause. However there is also an upward pointing part of the vertical motion in the lower mesosphere adiabatically cooling this region at the same time. The theoretically described cooling in the lower mesosphere was, to the authors

25 knowledge, first reported by Meriwether and Gerrard (2004) during a STE above Sondrestrom in Greenland (67°N, 309°E) in December 2000. This cooling can be confirmed for mean STE by our lidar measurements at both locations as well as by the MERRA-2 reanalysis data (cf. Fig. 2 and 3). This is in agreement with the study of Greer et al. (2013) investigating the mean characteristics of USLM disturbances. Note that the cooling is stronger at polar than at mid-latitudes, presumably because mid latitudes are if at all at the edge of the polar vortex and thus less affected because the downwelling is located in the center of

30 the polar vortex.

The dominating role of PWs in the stratosphere has long been known (e.g., Andrews et al., 1987; Plumb, 1989; Rosenlof and Holton, 1993). Our study quantitatively shows their impact on local measurements. With this new knowledge and the concept of local displacement, local measurements can be better brought into the global context. Additionally, effects which are not

based on PW variability can be much better identified and thus investigated. For example, in winter 1994/95 around day 25 (see supplements) there is a strong temperature enhancement at the stratopause where the original time series is about 17 K higher than the reconstructed time series based on wave 1, 2 and 3. This STE lies shortly before a SSW but in contrast to other STEs, as for example those reported by von Zahn et al. (1998) and Meriwether and Gerrard (2004) (cf. supplement), the agreement

5 with the PW variability is much lower and thus other effects seem to play a role. However it is not the scope of this study to investigate or discuss this unknown effect but with the help of the local displacement concept it can be better identified.

5 Summary

In this study we wanted to quantify the amount of quasi stationary PWs contributing to the day-to-day variability of the stratopause in northern hemisphere winter. Therefore we combine local lidar measurements at mid- and high latitudes with

10 global MERRA-2 reanalysis data to bring the local variability into the global context. With the help of stratopause temperature enhancements (STEs) the good agreement between local lidar measurements at Kühlungsborn (54°N, 11°E) and Andenes (69°N, 16°E) and the global MERRA-2 reanalysis data around the stratopause is shown. For example, both data sets show a lower stratopause in Kühlungsborn than in Andenes in their climatology as well as during STEs and a lower stratopause during STEs compared to its respective climatology.

15 Using MERRA-2 reanalysis data at the two designated latitudes and locations and applying the concept of local PW displacement it is shown that 98% (97%) of the local day-to-day stratopause temperature variability at Andenes (Kühlungsborn) can be explained by the variability of global PWs with wave numbers 1, 2 and 3. Thus PWs highly dominate the day-to-day variability of the stratopause at mid- and high latitudes in the northern hemisphere.

Data availability. MERRA-2 data are freely available from the MERRA project at https://gmao.gsfc.nasa.gov/reanalysis/MERRA-2/. Lidar

20 data are available from the corresponding author upon request.

Author contributions. RE and VM led the study and wrote the paper. RE also contributed to the lidar data collection and analysis, and to the interpretation of the results. VM analysed the MERRA-2 data, performed the wave analysis and interpreted the results. GB is responsible for and analysed the lidar measurements at Andenes. MG is responsible for lidar measurements at Kühlungsborn. JH provided the database for the lidar measurements. All authors read and approved the final manuscript.

25 *Competing interests.* The authors declare that they have no conflict of interest.

Acknowledgements. We thank Axel Gabriel for very helpful discussions. We would like to thank the people at the National Aeronautics and Space Administration (NASA, USA) for providing MERRA-2 data. This work was partly supported by the DFG project 218499286 (MS-GWaves/PACOG) which is part og the DFG researcher group FOR 1898 (MS-GWaves).

References

Alpers, M., Eixmann, R., Fricke-Begemann, C., Gerding, M., and Höffner, J.: Temperature lidar measurements from 1 to 105 km altitude using resonance, Rayleigh, and Rotational Raman scattering, Atmos. Chem. Phys., 4, 793–800, https://doi.org/10.5194/acp-4-793-2004, 2004.

5 Andrews, D. G., Holton, J. R., and Leovy, C. B.: Middle atmosphere dynamics, Academic Press, 1987.

Baldwin, M. P., Dunkerton, T. J., Baldwin, M. P., and Dunkerton, T. J.: Stratospheric Harbingers of Anomalous Weather Regimes Strato-spheric Harbingers of Anomalous Weather Regimes, Science (80-.)., 294, 581 – 584, https://doi.org/10.1126/science.1063315, 2001.

Baumgarten, G.: Doppler Rayleigh/Mie/Raman lidar for wind and temperature measurements in the middle atmosphere up to 80 km, Atmos. Meas. Tech., 3, 1509–1518, https://doi.org/10.5194/amt-3-1509-2010, 2010.

10 Bosilovich, M. G., Akella, S., Coy, L., Richard Cullather, Draper, C., Gelaro, R., Kovach, R., Liu, Q., Molod, A., Norris, P., Wargan, K., Chao, W., Reichle, R., Takacs, L., Vikhliaev, Y., Bloom, S., Collow, A., Stacey Firth, Gordon Labow, Partyka, G., Pawson, S., Reale, O., Schubert, S. D., and Suarez, M.: MERRA-2: Initial Evaluation of the Climate, Tech. Rep. Ser. Glob. Model. Data Assim., 43, https://gmao.gsfc.nasa.gov/pubs/docs/Bosilovich803.pdf, 2015.

Braesicke, P. and Langematz, U.: On the occurrence and evolution of extremely high temperatures at the polar winter stratopause - A GCM
15 study, Geophys. Res. Lett., 27, 1467–1470, https://doi.org/10.1029/2000GL011431, 2000.

Chanin, M.-L. and Hauchecorne, A.: Lidar observation of gravity and tidal waves in the stratosphere and mesosphere, J. Geophys. Res., 86, 9715–9721, https://doi.org/10.1029/JC086iC10p09715, 1981.

Charney, J. G. and Drazin, P. G.: Propagation of planetary-scale disturbances from the lower into the upper atmosphere, J. Geophys. Res., https://doi.org/10.1029/JZ066i001p00083, 1961.

20 Fairlie, T. D., Fisher, M., and O'Neill, A.: The development of narrow baroclinic zones and other small-scale structure in the stratosphere during simulated major warmings, Q. J. R. Meteorol. Soc., 116, 287–315, https://doi.org/10.1002/qj.49711649204, 1990.

Fritts, D. C. and Alexander, M. J.: Gravity wave dynamics and effects in the middle atmosphere, Rev. Geophys., 41, 1–64, https://doi.org/10.1029/2001RG000106, 2003.

Garcia, R. R. and Boville, B. A.: "Downward Control" of the Mean Meridional Circulation and Temperature Distribution of the Polar Winter
25 Stratosphere, J. Atmos. Sci., 51, 2238 – 2245, https://doi.org/10.1175/1520-0469(1994)051<2238:COTMMC>2.0.CO;2, 1994.

Gelaro, R., McCarty, W., Suárez, M. J., Todling, R., Molod, A., Takacs, L., Randles, C. A., Darmenov, A., Bosilovich, M. G., Reichle, R., Wargan, K., Coy, L., Cullather, R., Draper, C., Akella, S., Buchard, V., Conaty, A., da Silva, A. M., Gu, W., Kim, G. K., Koster, R., Lucchesi, R., Merkova, D., Nielsen, J. E., Partyka, G., Pawson, S., Putman, W., Rienecker, M., Schubert, S. D., Sienkiewicz, M., and Zhao, B.: The modern-era retrospective analysis for research and applications, version 2 (MERRA-2), J. Clim., 30, 5419–5454,
30 https://doi.org/10.1175/JCLI-D-16-0758.1, 2017.

Gerding, M., Höffner, J., Lautenbach, J., Rauthe, M., and Lübken, F.-J.: Seasonal variation of nocturnal temperatures between 1 and 105km altitude at 54°N observed by lidar, Atmos. Chem. Phys., 8, 7465–7482, https://doi.org/10.5194/acp-8-7465-2008, 2008.

Greer, K., Thayer, J. P., and Harvey, V. L.: A climatology of polar winter stratopause warmings and associated planetary wave breaking, J. Geophys. Res. Atmos., 118, 4168–4180, https://doi.org/10.1002/jgrd.50289, 2013.

35 Haynes, P. H., Marks, C., McIntyre, M. E., Shepherd, T. G., and Shine, K. P.: On the "Downward Control" of the Extratrop-ical Diabatic Circulations by Eddy-Induced Mean Zonal Forces, J. Atmos. Sci., 48, 651 – 678, https://doi.org/10.1175/1520-0469(1991)048<0651:OTCOED>2.0.CO;2, 1991.

Hitchman, M., Gille, J., Rodgers, C., and Brasseur, G.: The Separated Polar Winter Stratopause: A Gravity Wave Driven Climatological Feature, J. Atmos. Sci., 46, 410 – 422, https://doi.org/10.1175/1520-0469, 1989.

Kodera, K., Mukougawa, H., and Itoh, S.: Trospheric impact of reflected planetary waves from the stratosphere, Geophys. Res. Lett., 35, 3–6, https://doi.org/10.1029/2008GL034575, 2008.

5 Kretschmer, M., Cohen, J., Matthias, V., Runge, J., and Coumou, D.: The different stratospheric influence on cold-extremes in Eurasia and North America, npj Clim. Atmos. Sci., 1, 44, https://doi.org/10.1038/s41612-018-0054-4, 2018.

Lindzen, R. S.: Turbulence and stress owing to gravity wave and tidal breakdown, J. Geophys. Res., 86, 9707, https://doi.org/10.1029/jc086ic10p09707, 1981.

Manney, G. L., Kru, K., Pawson, S., Minschwaner, K., Schwartz, M. J., Daffer, W. H., Livesey, N. J., Mlynczak, M. G., Remsberg, E. E., Iii,
10 J. M. R., and Waters, J. W.: The evolution of the stratopause during the 2006 major warming : Satellite data and assimilated meteorological analyses, J.Geophys. Res., 113, 1–16, https://doi.org/10.1029/2007JD009097, 2008.

Matsuno, T.: Vertical Propagation of Stationary Planetary Waves in the Winter Northern Hemisphere, J. Atmos. Sci., 27, 871–883, https://doi.org/10.1175/1520-0469(1970)027<0871:vpospw>2.0.co;2, 1970.

Matsuno, T.: A Dynamical Model of the Stratospheric Sudden Warming, J. Atmos. Sci., 28, 1479–1494, https://doi.org/10.1175/1520-
15 0469(1971)028<1479:admots>2.0.co;2, 1971.

Matthias, V., Hoffmann, P., Rapp, M., and Baumgarten, G.: Composite analysis of the temporal development of waves in the polar MLT region during stratospheric warmings, J. Atmos. Solar-Terrestrial Phys., 90-91, https://doi.org/10.1016/j.jastp.2012.04.004, 2012.

McIntyre, E. M. and Palmer, N.: Breaking planetary waves in the stratosphere, Nature, 305, 593–600, https://doi.org/10.1038/305593a0, 1983.

20 Meriwether, J. W. and Gerrard, A. J.: Mesosphere inversion layers and stratosphere temperature enhancements, Rev. Geophys., 42, 1–31, https://doi.org/10.1029/2003RG000133, 2004.

Molod, A., Takacs, L., Suarez, M., and Bacmeister, J.: Development of the GEOS-5 atmospheric general circulation model: Evolution from MERRA to MERRA2, Geosci. Model Dev., 8, 1339–1356, https://doi.org/10.5194/gmd-8-1339-2015, 2015.

Picone, J. M., Hedin, A. E., Drob, D. P., and Aikin, A. C.: NRLMSISE-00 empirical model of the atmosphere: Statistical comparisons and
25 scientific issues, J. Geophys. Res. Sp. Phys., 107, 1–16, https://doi.org/10.1029/2002JA009430, 2002.

Plumb, R. A.: On the seasonal cycle of stratospheric planetary waves, Pure Appl. Geophys. PAGEOPH, 130, 233–242, https://doi.org/10.1007/BF00874457, 1989.

Plumb, R. A.: Stratospheric Transport, J. Meteorol. Soc. Japan. Ser. II, 80, 793–809, https://doi.org/10.2151/jmsj.80.793, 2002.

Rind, D., Shindell, D., Lonergan, P., and Balachandran, N. K.: Climate change and the middle atmosphere. Part III: the doubled CO2 climate
30 revisited, J. Clim., 11, 876–894, https://doi.org/10.1175/1520-0442(1998)011<0876:CCATMA>2.0.CO;2, 1998.

Rosenlof, K. and Holton, J. R.: Estimates of the Stratospheric Residual Circulation Using the Downward Principle, J. Geophys. Res., 98, 10 465 – 10 479, https://doi.org/10.1029/93JD00392, 1993.

Schöch, A., Baumgarten, G., and Fiedler, J.: Polar middle atmosphere temperature climatology from Rayleigh lidar measurements at ALO-MAR (69° N), Ann. Geophys., 26, 1681–1698, https://doi.org/10.5194/angeo-26-1681-2008, 2008.

35 Thayer, J. P., Greer, K., and Harvey, V. L.: Front-like behavior in the Arctic wintertime upper stratosphere and lower mesosphere, J. Geophys. Res. Atmos., 115, 1–10, https://doi.org/10.1029/2010JD014278, 2010.

von Zahn, U., Fiedler, J., Naujokat, B., Langematz, U., and Krüger, K.: A note on record-high temperatures at the northern polar stratopause in winter 1997/98, Geophys. Res. Lett., 25, 4169–4172, https://doi.org/doi:10.1029/1998GL900091, 1998.
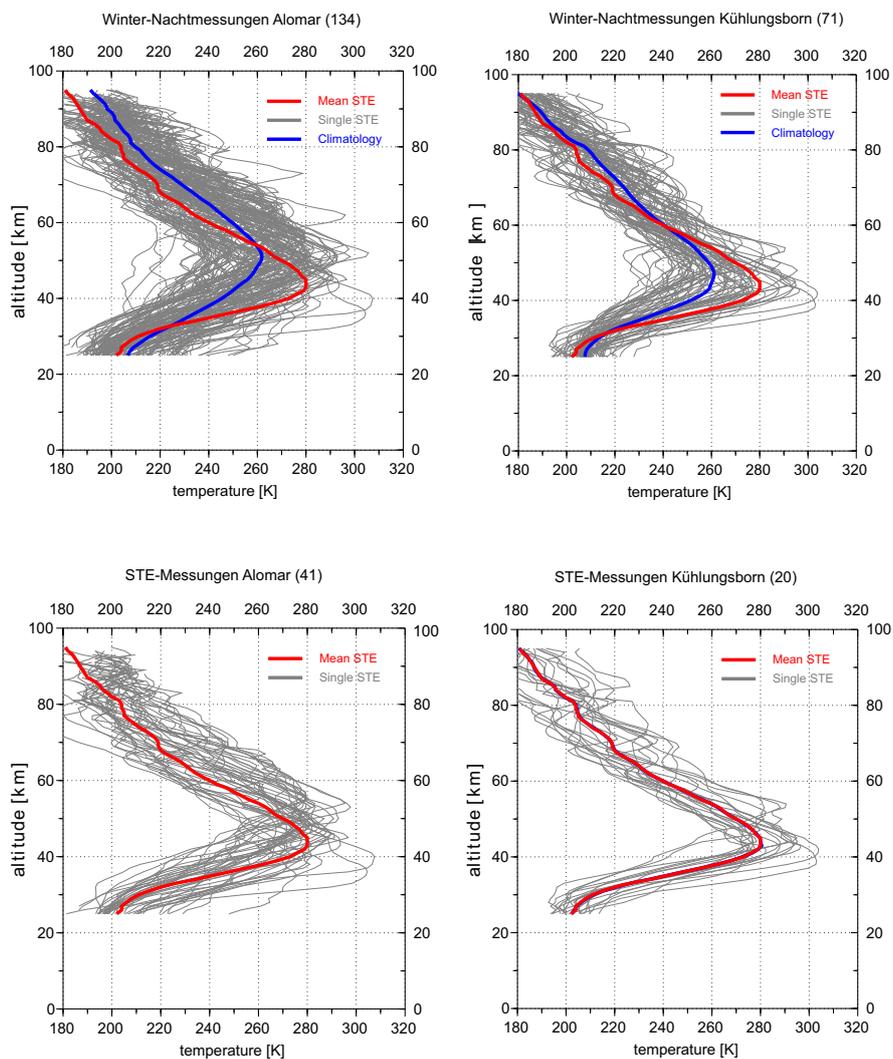
Figure 2. a+b) Vertical profiles (blue lines) of all nighttime lidar temperature measurements between 2002 and 2012 at Andenes (a) and Kühlungsborn (b) and their respective long-term mean (red line). c+d) Same as in the top row but only for those nights where a STE is detected at 2 hPa. Note that the error bars on the long-term mean denote only atmospheric variance. In contrast, measurement errors are negligible.
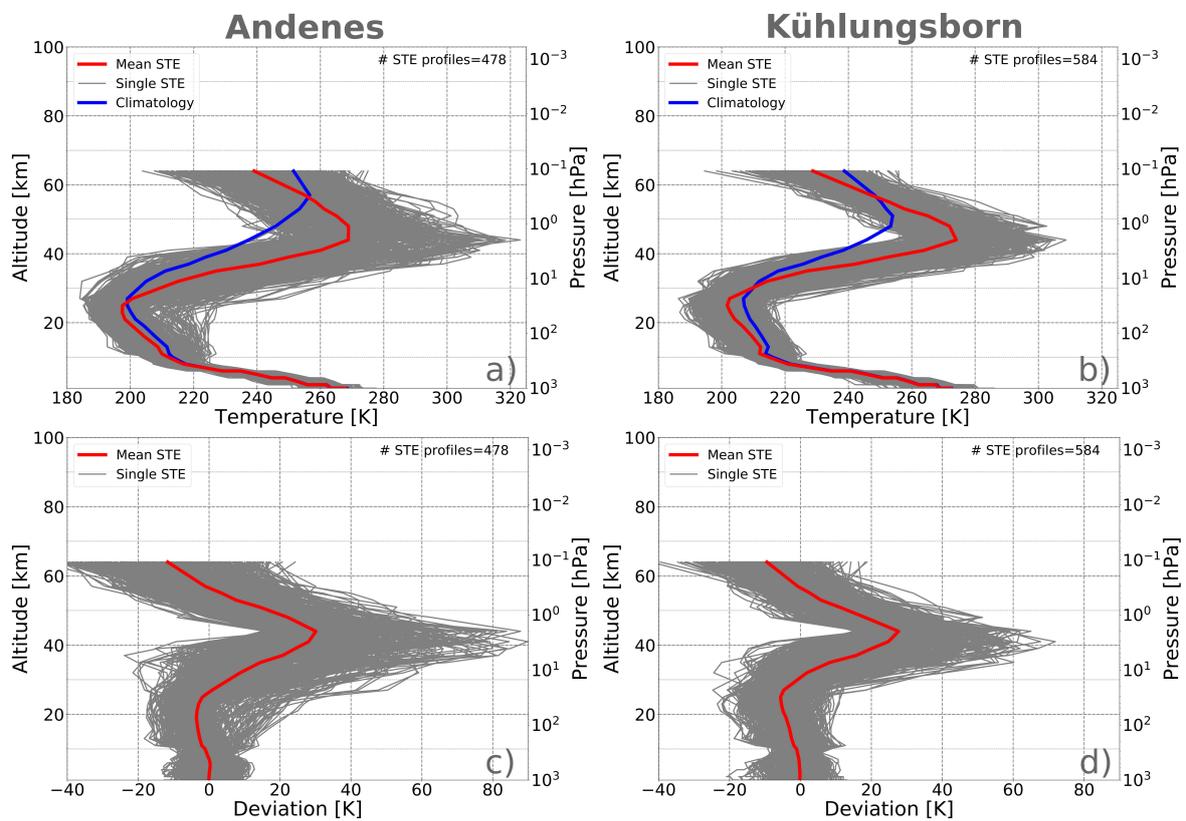
Figure 3. a+b) Vertical profiles (grey) of all STEs between winter 1980/81 and 2018/19 in MERRA-2 data at Andenes and Külungsborn and their respective long-term mean (red line). The blue line represents the climatology over all winter profiles. c+d) Same as in the top row but the long-term mean is subtracted.
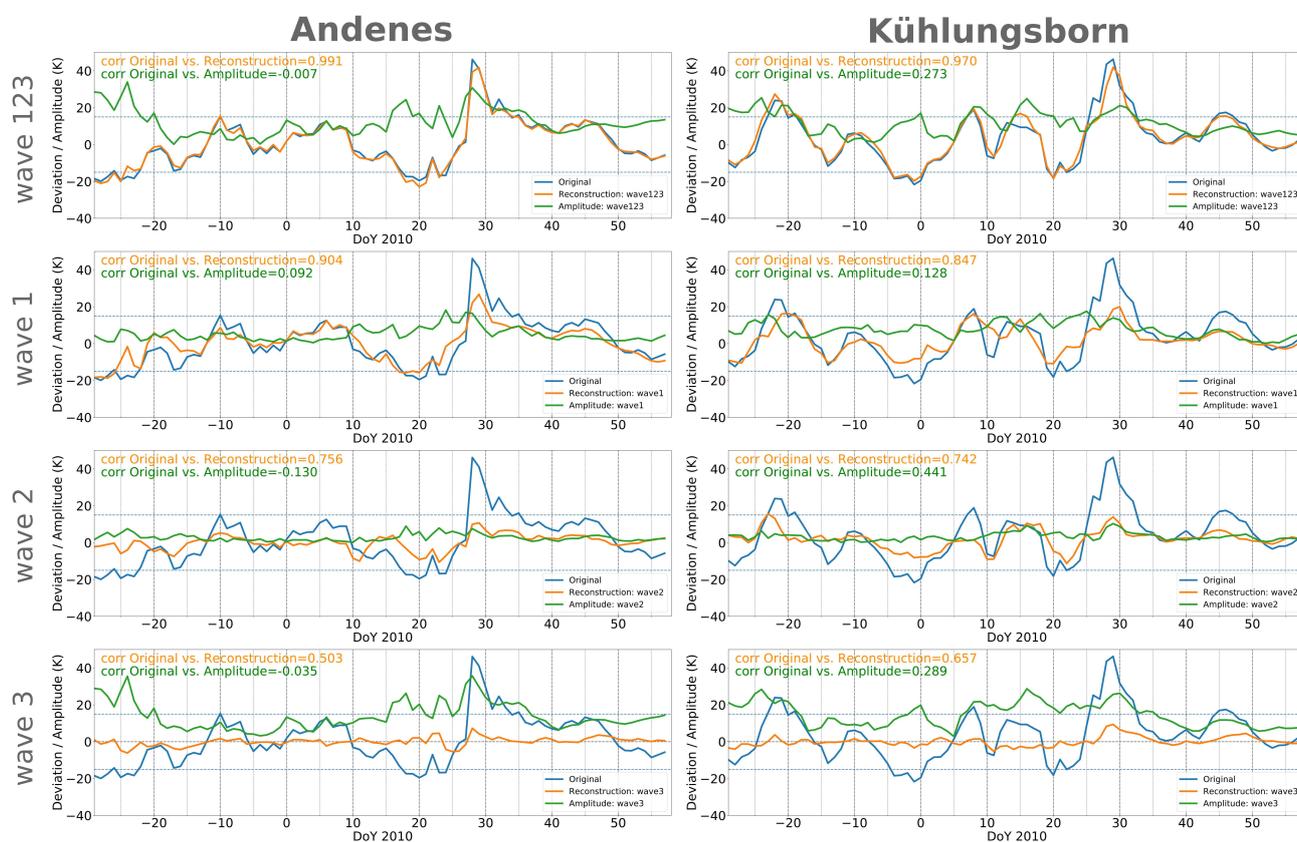
Figure 4. Temporal evolution of the temperature deviation from the climatological daily mean at Andenes (left) and Kühlungsborn (right) at 2 hPa (blue line). The amplitude of each individual wave number (different rows) is represented by the green lines while the local displacement, also called reconstructed time series, is represented by the orange lines. The horizontal grey dashed lines mark the positive and negative threshold of a STE. All data presented here are derived from MERRA-2 data.